# Overview of CMOS process and design options for image sensor dedicated to space applications

P. Martin-Gonthier*, P.Magnan**, F. Corbiere***

SUPAERO – Integrated Image Sensors Laboratory
10 avenue Edouard Belin, 31400 Toulouse, France

## ABSTRACT

With the growth of huge volume markets (mobile phones, digital cameras…) CMOS technologies for image sensor improve significantly. New process flows appear in order to optimize some parameters such as quantum efficiency, dark current, and conversion gain. Space applications can of course benefit from these improvements. To illustrate this evolution, this paper reports results from three technologies that have been evaluated with test vehicles composed of several sub arrays designed with some space applications as target. These three technologies are CMOS standard, improved and sensor optimized process in 0.35µm generation. Measurements are focussed on quantum efficiency, dark current, conversion gain and noise. Other measurements such as Modulation Transfer Function (MTF) and crosstalk are depicted in [1]. A comparison between results has been done and three categories of CMOS process for image sensors have been listed. Radiation tolerance has been also studied for the CMOS improved process in the way of hardening the imager by design. Results at 4, 15, 25 and 50 krad prove a good ionizing dose radiation tolerance applying specific techniques.

**Keywords:** CMOS Image Sensors, Quantum efficiency, Dark current, Conversion gain, Radiation tolerance

## 1. INTRODUCTION

CMOS image sensors are nowadays extensively considered for several space applications. However, missions requirements may vary considerably in term of spectral band, flux amount, charge handling capacity and signal to noise ratio [2]. This paper will demonstrate that several CMOS process and design options are now available to fulfill most of these multiple requirements.

CMOS standard processes, which are developed for digital and mixed signal applications, are really attractive particularly because of their low power consumption, applicability for on-chip signal processing and large availability. However, electro-optic performances are often inadequate for high end applications. Several studies [3] [4] [5] show the best ways to improve image sensor performances. Use of deep Pwell allows to improve photosensitivity and spectral response as well as crosstalk. P on P+ epitaxial substrate can also be used to increase photosensitivity and spectral response by improving direct collection notably for long wavelengths. Additional back ends as antireflective film also improve response of image sensors. Other ways are use of depletion transistor for reset transistor or double metal photoshield for crosstalk and blooming improvement. These modifications brought to standard process unavoidably increase fabrication complexity and costs.

Section 2 of the paper gives an overview of various CMOS image sensor test vehicles designed by SUPAERO-CIMI team using three different 0.35µm technologies - standard, improved and image sensor optimized (CIS) CMOS process - representative of two level of efforts done in order to meet image sensor requirements.

* philippe.martin_gonthier@supaero.fr; phone +33 5 62 17 83 69; fax +33 5 62 17 83 45
** pierre.magnan@supaero.fr; phone +33 5 62 17 80 79; fax +33 5 62 17 83 45
*** franck.corbiere@supaero.fr; phone +33 5 62 17 82 96; fax +33 5 62 17 83 45

Copyright 2005 Society of Photo-Optical Instrumentation Engineers. This paper was published in "Proceedings of SPIE - Volume 5978 - Sensors, Systems, and Next-Generation Satellites IX" and is made available as an electronic reprint with permission of SPIE. One print or electronic copy may be made for personal use only. Systematic or multiple reproduction, distribution to multiple locations via electronic or other means, duplication of any material in this paper for a fee or for commercial purposes, or modification of the content of the paper are prohibited.

These test vehicles are composed of various sub-arrays with different pixel types. All pixels are 3T structures with a closed pitch (13 and 15µm). A description of the key features of the technologies and pixel organization will be given to illustrate the elements of the trade-off in the selection and optimization process.
In section 3, characterization results are presented for these three technologies with a special interest for three key parameters: quantum efficiency, dark current and conversion gain. These parameters give an overview of performances and highlight the impact of both process and design option.
Section 4 focuses on radiation tolerance. Effects of radiation will be considered for both the technology level (intrinsic radiation behavior) and the design level for the impact of pixel type and organization (standard and radhard design).
In conclusion of the paper, a summary of key benefits of the various approaches will be presented.

## 2. DESCRIPTION OF TEST VEHICLES AND TECHNOLOGIES

In this section, test vehicles are described with different pixel structures and key features of the three technologies used are given. Awaited benefits and drawbacks of using pixel structures and technologies are depicted.

All pixels in this paper are 3T structures as shown in figure 1. At the beginning of a line period, the photodiode is "reset" by transistor T1. Reference level is carried out by the follower transistor (T2) and selection row switch (T3) and sampled at the bottom of the column. During integration time, photodiode is in self-integrating mode (integrating charges in its own capacitance). At the end of integration, signal is read out through the follower transistor and selection row switch and sampled; then another cycle (next frame) can start.

For all 3T pixel type structures in different technologies, reset noise is dominant because only Differential Double Sampling is performed (correlated double sampling non available). In soft reset mode [6] [7], reset noise (in electron) can be estimated as:

$$\sigma_{RESET} \approx \sqrt{KTC_{Ph}/2} \text{ (electrons)} \quad \text{where } C_{Ph} \text{ is the photodiode capacitance}$$

Thus, in first approximation, global noise is a function of detection node capacitance.

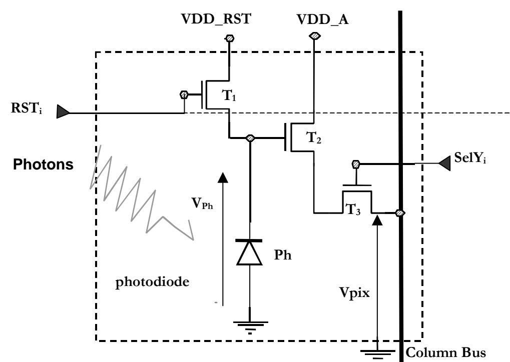


Figure 1 : 3T pixel type

### 2.1 AMIS 0.35µm test vehicle

The development of this vehicle was supported by the French National Space Agency CNES (Centre National d'Etudes Spatiales) under contract N°719/CNES/01/8631/00 [8].

The AMIS 0.35µm 2P/5M technology is an analog standard process derived from core process (digital process). No improvements were made for image sensors. It is an epitaxial technology (several µm thickness for epitaxial layer) on an heavily doped substrate.

Test vehicle is a 250x200 array composed of 11 sub arrays. Only 3 sub arrays (100x50) are reported in this paper. Figure 2 a) shows a microphotograph of the chip with the location of the sub arrays. All pixels in these sub-arrays have a 3T structure with a 15 µm pitch. Only their photosensitive area structures are different. The corresponding vertical cross-sections are shown in figure 2 b), c) and d).

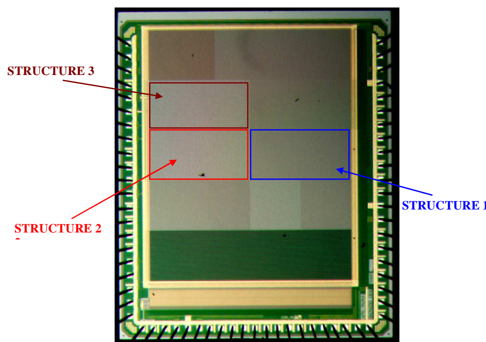


a) Microphotograph and sub-arrays location

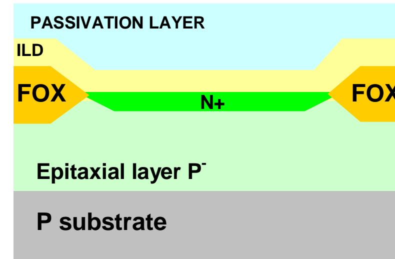


b) Structure 1: 3T N+
(geometrical fill factor: 67%)

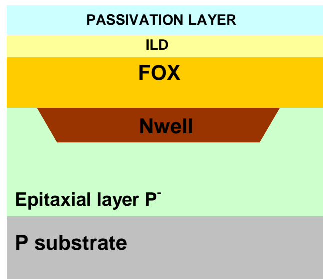


c) Structure 2 : 3T Nwell
(geometrical fill factor: 67%)

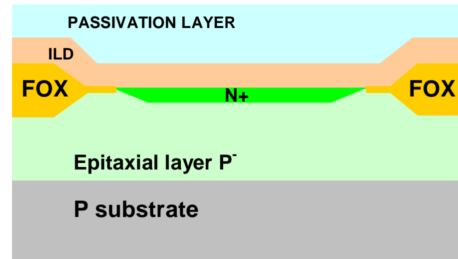


d) Structure 3 : 3T N+. N+ diffusion with No FOX at edges
(geometrical fill factor: 50%)

Figure 2 : Microphotograph and photosensitive area of AMIS 0.35µm test vehicle (15µm pixel pitch)

Structure 1 has a photosensitive area designed with N+ diffusion over $P_{EPI}$. This pixel is the baseline structure for this technology. Structure 2 is designed with Nwell/ $P_{EPI}$ diode for photosensitive area. Using Nwell diode has three impacts: improve direct collection of photons by enlarged depletion region, reduce capacitance of photosensitive area due to dopage level of Nwell and minimize dark current by avoiding surface stress on structure. Structure 3 is designed with N+ diffusion for photosensitive area. Field oxide (FOX) is patterned aside of N+ diffusion to avoid bird's beak proximity and thus to minimize dark current.

### 2.2 AMS OPTO 0.35µm test vehicle

This vehicle was designed with the support of EADS-Astrium in order to evaluate radiation tolerance and design options.

The AMS OPTO 0.35µm 2P/3M technology is an analog standard process derived from core process (digital process) and improved for image sensors. Improvements are in two ways: using a deeper epitaxial layer than for AMIS and having an antireflective coating and an optimization of superficial layers (passivation) in order to minimize interference effects.

Test vehicle is a 128x256 array composed of 10 sub-arrays. Only 3 sub-arrays (one of 64x32 and two of 64x64) are considered in this paper. Figure 3 a) shows a microphotograph of the chip with the location of the sub arrays. All pixels in these sub arrays have a 3T structure with a 15µm pitch. Only photosensitive area types and/or constructions are different. Test vehicle was designed to evaluate ionizing dose radiation tolerance. Thus, readout circuits are designed with ELT (Enclosed Layout Transistors) MOS [9]. Row and column decoder circuits also make use of ELT MOS to avoid any degradation of the digital part. The study focussed on pixel radiation tolerance. Section 4 will give results on radiation tolerance. These structures (vertical cut) are shown in Figure 3 b), c), and d).

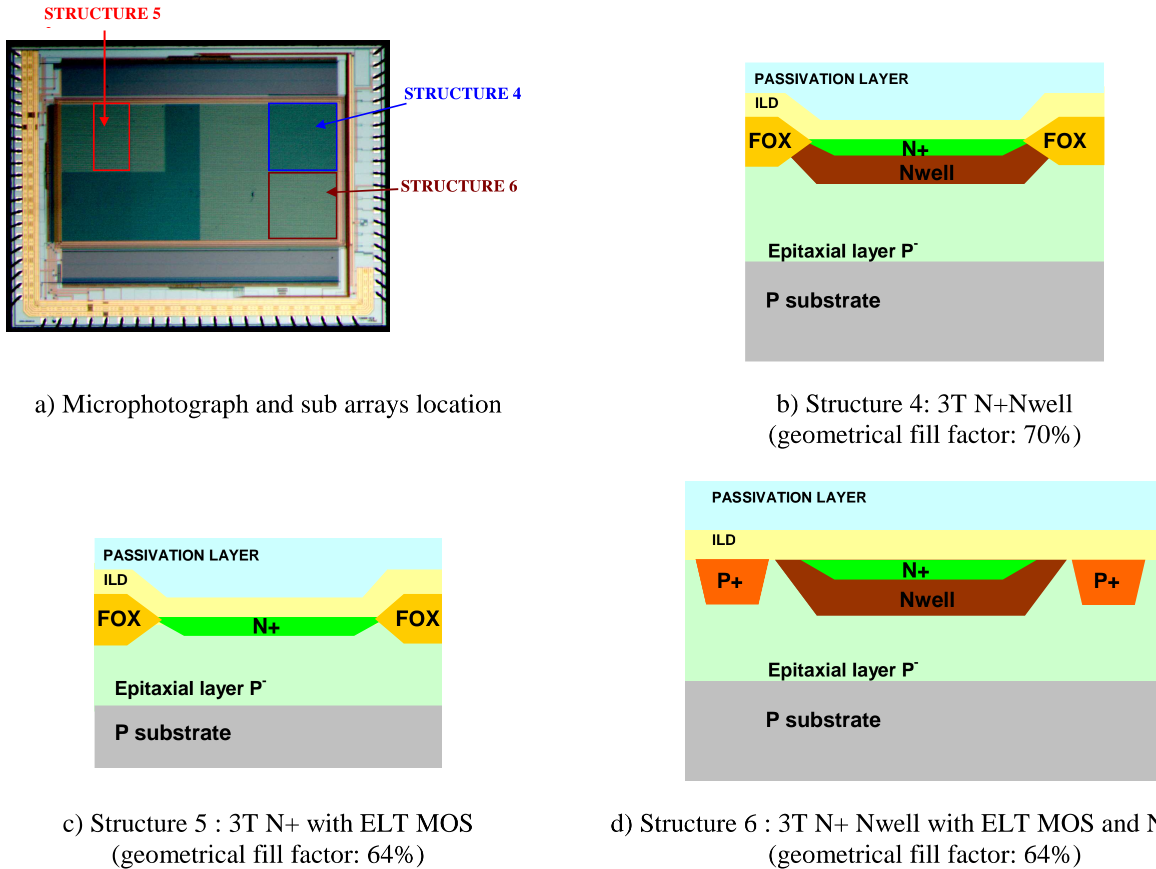


a) Microphotograph and sub arrays location

b) Structure 4: 3T N+Nwell (geometrical fill factor: 70%)

c) Structure 5 : 3T N+ with ELT MOS (geometrical fill factor: 64%)

d) Structure 6 : 3T N+ Nwell with ELT MOS and No FOX (geometrical fill factor: 64%)

Figure 3 : Microphotograph and photosensitive area of AMS OPTO 0.35µm test vehicle (15µm pixel pitch)

Structure 4 has a photosensitive area designed with N+ and Nwell diffusion as recommended by AMS to get the best pixel. This pixel is the baseline structure for this technology. It has no ELT MOS in readout circuit. Structure 5 is designed with N+ diffusion for photosensitive area and ELT MOS. In addition, guard rings are designed around sensitive area and transistors to avoid leakage current created by radiations. Structure 6 is designed with N+ and Nwell diffusion for photosensitive area. Field oxide (FOX) is excluded from the pixel. Guard rings are designed to avoid leakage current due to radiations. These two last structures are designed to test radiation tolerance.

### 2.3 UMC CIS 0.35µ test vehicle

This vehicle was designed with the support of EADS-Astrium.

The UMC CIS (CMOS Image Sensor) 0.35µm 2P/3M technology is an analog standard process derived from core process (digital process). Strong optimizations are made to improve performances of image sensors in terms of quantum efficiency and dark current. Additional masks are used to build the pixel compared to AMS and AMIS processes. These

masks allow for dedicated doping profile of the photodiode and this process optimizes the top layer stack for enhanced transmission.

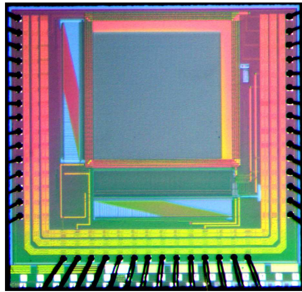

a) Microphotograph

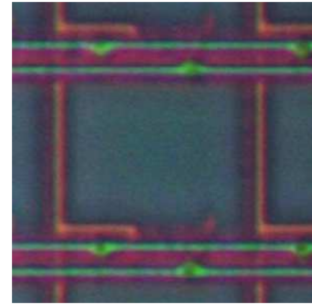

c) Pixel view (geometrical fill factor: 61%)

Figure 4 : Microphotography and pixel view of UMC CIS 0.35µm test vehicle (13µm pixel pitch)

Test vehicle is a 128x128 array composed of one type of structure. Figure 4 a) shows a microphotography of the chip. View of the pixel is shown in figure 4 b). Pixel structure (called Structure 7) is a 3T and has a photosensitive area build on a lightly doped substrate left in the pixel area.

Section 3 synthesizes main measurement results on these pixel structures and technologies.

## 3. MEASUREMENT RESULTS AND COMPARISON

Same measurements were made for the three test vehicles with the same characterization setup. During measurements, temperature of test vehicles was regulated to 20°C except for dark current measurements done at 20 and 10°C.

### 3.1 AMIS 0.35µm technology

Figure 5 depicts quantum efficiency of structure 1, 2 and 3. A light increase of quantum efficiency at short wavelengths (400-450nm) is noted between N+ diffusion (structure 1) and Nwell diffusion (structure 2). There is a more significant difference in quantum efficiency results between Structure 1 and Structure 3 due to N+ diffusion area reduction (spacing of the FOX).

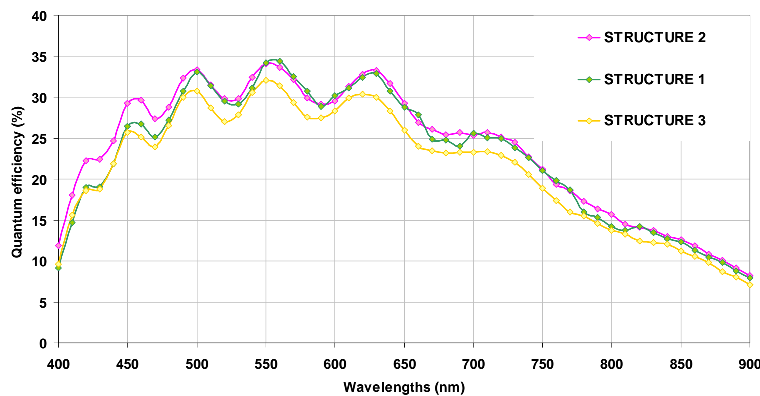


Figure 5 : Quantum efficiency of AMIS 0.35µm process structures

Table 1 gives measurement results concerning the 3 structures AMIS 0.35µm process test vehicle.

| | Peak Quantum Efficiency | Conversion gain (µV/e⁻) | Dark current (nA/cm²) | | Noise in rms electron |
|---|---|---|---|---|---|
| | | | 10 °C | 20°C | |
| **Structure 1** | 35 % | 1.13 | 0.25 | 0.53 | 111 |
| **Structure 2** | 34 % | 5.20 | 0.08 | 0.19 | 39 |
| **Structure 3** | 32 % | 1.79 | 0.18 | 0.43 | 81 |

Table 1 : Measurements results for AMIS test vehicle's structures

Table 1 shows measured conversion gains. Structure 2 gives excellent results in term of dark current (190 pA/cm² at 20 °C). Compared to structure 1, structure 3 gives satisfaction by reducing dark current (bird's beak removed). It appears that noise is strongly dependent of detection node capacitance (soft reset mode) and results fit with expected trend (decrease of temporal noise level in electron with increase of conversion gain). Respectively for structure 1, 2 and 3, carried out noise is 121, 56 and 96 electron rms.

### 3.2 AMS OPTO 0.35µ Technology

Quantum efficiency curves of structure 4, 5 and 6 of AMS OPTO 0.35µm process are depicted in figure 6. Structures with Nwell photodiode (4 and 6) strongly improve quantum efficiency due to a better charge collection (greater depletion area) and antireflective film. Peak quantum efficiency for these two structures is around 43 % at 694nm. In comparison, for the structure with only N+ diffusion (structure 5), peak quantum efficiency is obtained for a shorter wavelength (500nm) and is about 29%.

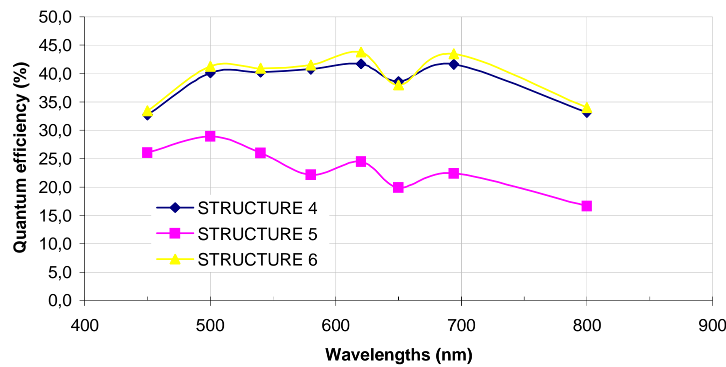


Figure 6 : Quantum efficiency for AMS OPTO 0.35µm process

Table 2 gives measurement results about the 3 structures for the test vehicle of AMS OPTO 0.35µm process.

| | Peak Quantum Efficiency | Conversion gain (µV/e) | Dark current (nA/cm²) | | Noise in rms electron |
|---|---|---|---|---|---|
| | | | 10 °C | 20°C | |
| **Structure 4** | 43 % | 5.78 | 0.17 | 0.405 | 30 |
| **Structure 5** | 29 % | 1.48 | 0.56 | 1.06 | 72 |
| **Structure 6** | 43 % | 4.60 | 1.76 | 4.314 | 56 |

Table 2 : Measurements results for AMS OPTO test vehicle's structures

As expected, conversion gains for structures built with Nwell (structures 4 and 6) are higher than the structure with only N+ diffusion (structure 5). So, high conversion gain with a 3T structure can be reached, even with large pixel pitch. Results of dark current for reference structure of this technology (structure 4) show medium value with 405 pA/cm² at 20°C. However, dark current of structure 5 and 6 are higher with, respectively, 1.06 nA/cm² and 4.314 nA/cm² at 20 °C. These structures were designed for radiation tolerance i.e to limit the DC degradation with the dose. Section 4 gives measurement results of these structures on ionizing radiation tolerance. Temporal noise levels in electron are low.

### 3.3 UMC CIS 0.35µ TECHNOLOGY

Figure 7 depicts quantum efficiency for structure 7 with UMC CIS 0.35µm process. Thanks to process optimization, peak quantum efficiency is about 46 % at 600nm (fill factor: 61%). Conversion gain is measured to 3.9 µV/$e^-$. Dark current at 10°C and 20°C are respectively of 80 pA/cm² and 200 pA/cm². A noise of 21 electrons rms was measured.

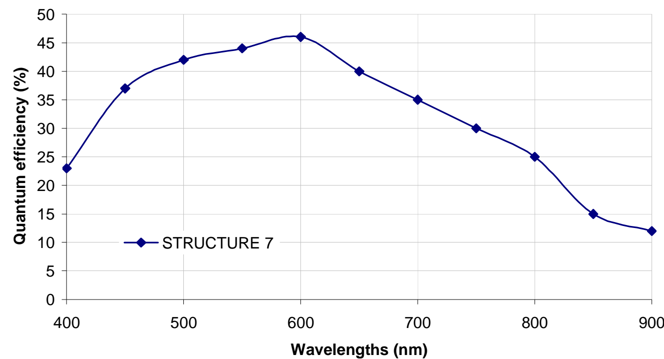


Figure 7 : Quantum efficiency for UMC CIS 0.35µm process structure

### 3.4 COMPARISON

A general remark is that temporal noise level measured in soft reset mode and low flux are very low for AMS OPTO and UMC CIS 0.35µm process. Investigations are going on to separate the different contributions (reset noise, source follower low frequency and thermal noise, sampling noise) .

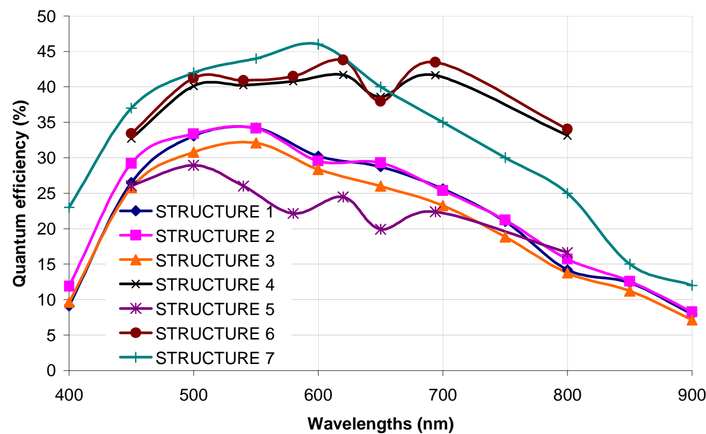


Figure 8 : Quantum efficiency comparison for the three technologies

Measurement results show that pixel design optimization can be made to improve pixel performance. Using Nwell in photosensitive area generally increases quantum efficiency (see figure 6) and avoids stress that causes increase of dark

current. Using Nwell also allows to increase conversion gain by minimizing capacitance (Nwell is lightly doped compared to N+ diffusion). With AMIS 0.35µm process, field oxide spacing (structure 3) allows to reduce dark current compared to structure 1 (reference structure in this technology) but this behavior appears to be process dependant.

Comparison between the three technologies (AMIS, AMS and UMC) demonstrates good performances for UMC CIS process not only in terms of quantum efficiency as depicted in figure 8, but also in term of dark current. AMS OPTO quantum efficiency decreases slower than UMC CIS for long wavelengths The AMS OPTO process antireflective film (optimized for long wavelengths) and the thicker EPI layer result in a significant improvement in NIR region of the spectrum. The difference in the quantum efficiency behavior at long wavelengths between these two processes is largely due to the thinner EPI used by UMC. For the standard process (AMIS), quantum efficiency is more limited but no optimization is performed. For detection node capacitance which determine the conversion gain in 3T configuration, the use of lightly doped N diffusion allows to have same performances for the three processes.

## 4. IONIZING RADIATION TOLERANCE

Radiation tolerance (total dose) was evaluated on AMS OPTO 0.35µm process. Structure 4 (3T N+Nwell) is the reference structure for this technology. Structures 5 (3T N+ with ELT MOS) and 6 (3T N+ Nwell with ELT MOS and No FOX) was designed to minimize degradation due to radiation.. Cobalt 60 irradiations were performed at ONERA Toulouse with a dose rate of 160 rad/h. Measurements were done for 4, 15, 25 and 50 krad radiation levels in a first step. Annealing was done at 80°C during one week for all irradiated parts. Measurements were taken with same conditions that previously described in section 3.

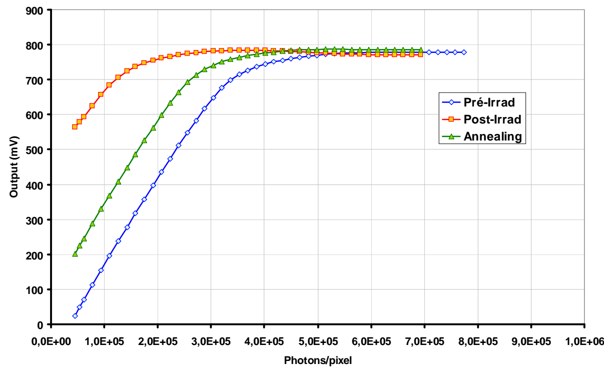


a) Structure 4

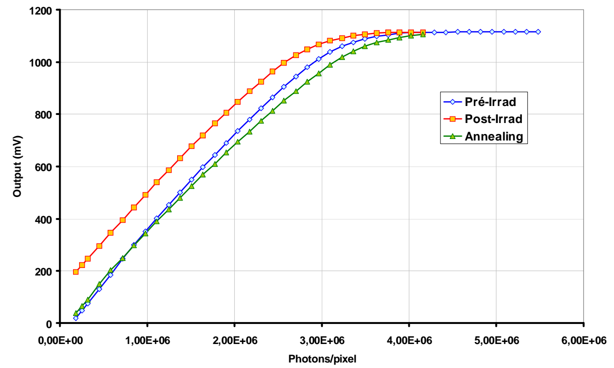


b) Structure 5

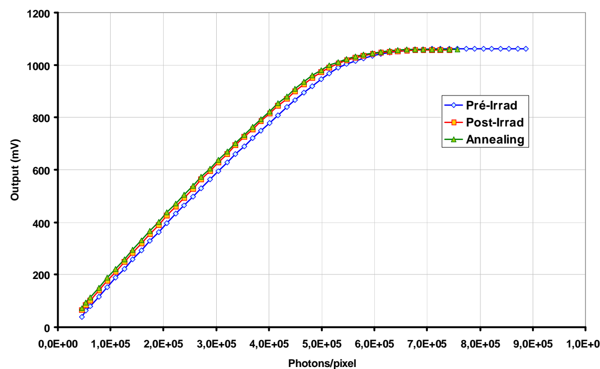


c) Structure 6

Figure 9 : Sensitivity curves pre-irradiation, post irradiation at 50krad and after annealing of structures 4, 5 and 6

Measurements are focussed on three parameters: quantum efficiency, conversion gain and dark current. Figure 9 shows sensitivity curves obtained with no irradiations, after 50krad irradiations and after annealing. For structures 4 and 6, slopes of the curves (which represent quantum efficiency multiplied by conversion gain) do not show evolution due to irradiation and annealing. Slopes of structure 5 features slight differences between them. These results allow to confirm that there is no major impact of ionizing radiation at least up to 50krad for quantum efficiency and conversion gain [10] [11].

Dark current results are depicted in figure 10 for various doses. For structure 4, which is the baseline structure, dark current before irradiation is 405 pA/cm². This value increases strongly with total dose received after annealing. No specific design was made for this structure. At 50 krad, dark current is multiplied by 68 compared to pre-irradiation as shown in figure 11. At each level dose corresponds a test vehicle, thus explaining slight variations of dark current in pre-irradiation. For structure 5, which is a N+ diffusion photodiode with hardened design, dark current without radiation is higher than structure 4: 1.06 nA/cm². However, increase of dark current is minimized. At 50 krad, after annealing, dark current is multiplied by 5.31 compared to pre-irradiation. Structure 6 has a dark current level of 4.31 nA/cm² before irradiation. At 50 krad, after annealing, dark current is multiplied by 2.33 compared to pre-irradiation.

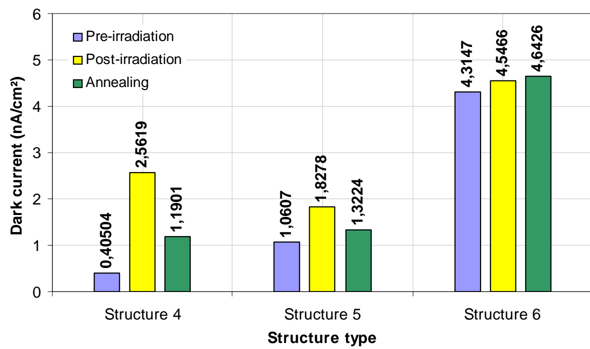


a) 4 Krad

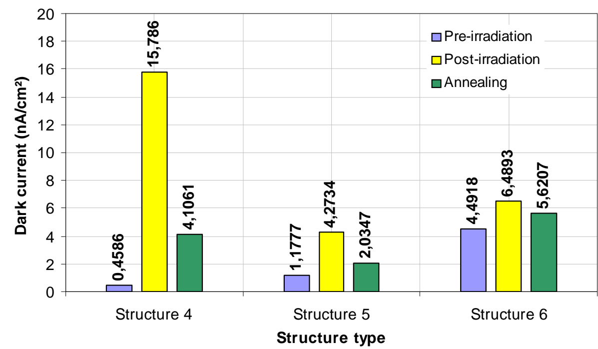


b) 15 Krad

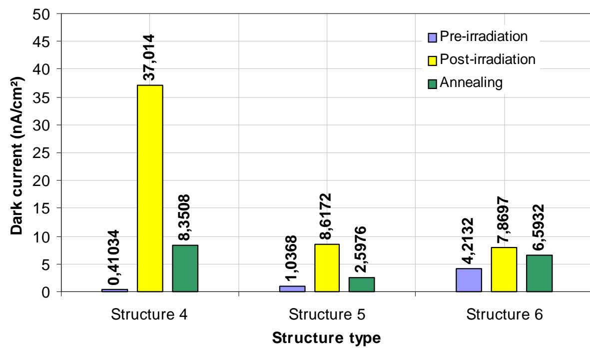


c) 25 Krad

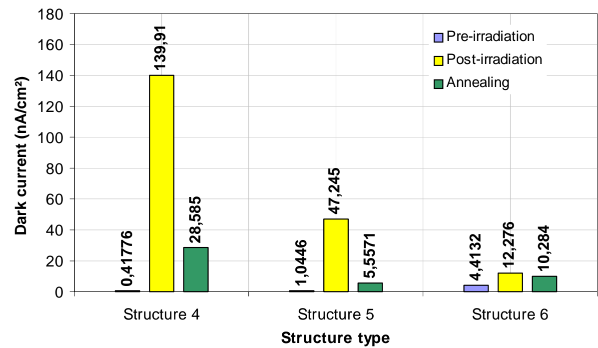


d) 50 Krad

Figure 10 : Dark current measurements for pre-irradiation, post-irradiation and after annealing for 4, 15, 25 and 50 krad ionizing dose

Structures 5 and 6 provide excellent results in terms of hardening. Indeed, dark current increase versus ionizing dose stays low.

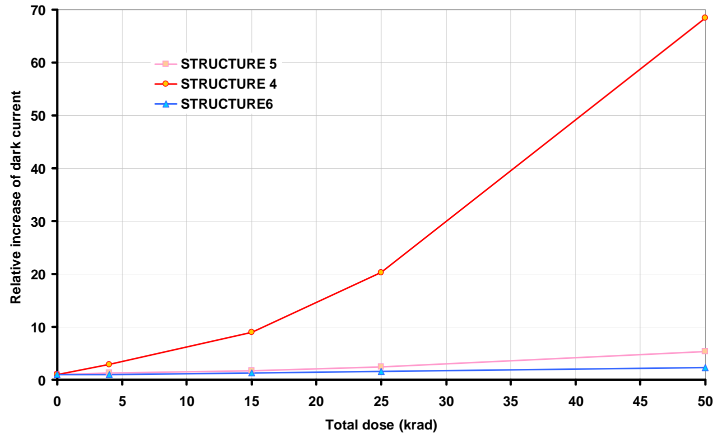


Figure 11 : Dark current relative increase vs total ionizing dose

Figure 12 a) shows an image grabbed with the sensor at 50krad. A test vehicle was irradiated at 100krad and characterizations will be done. However, an image was grabbed at 100krad without annealing to prove the good behavior of the test vehicle as shown in figure 12 b).

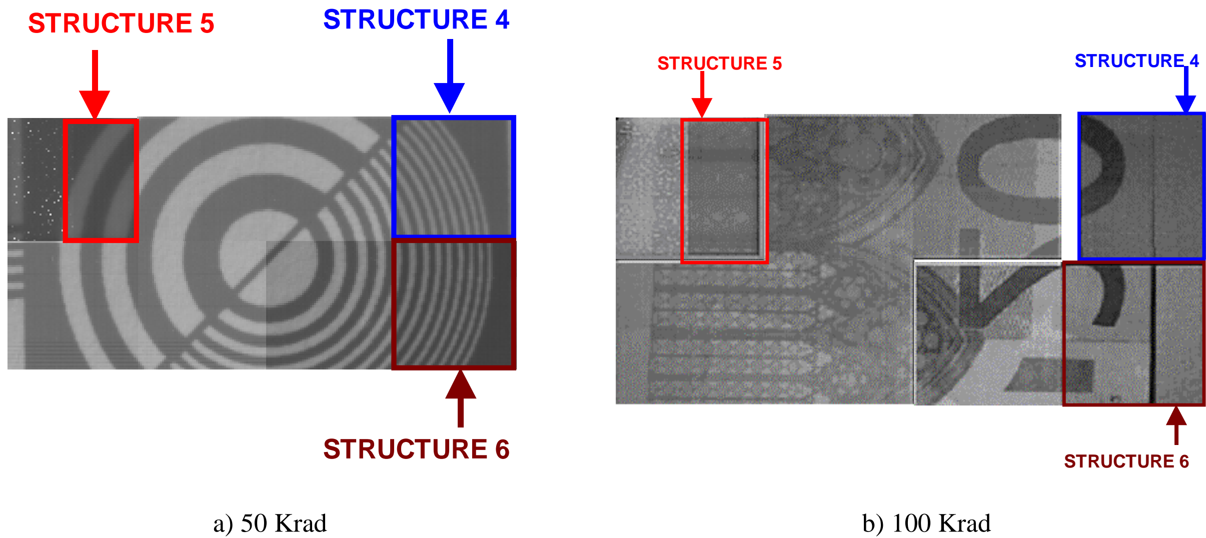


a) 50 Krad

b) 100 Krad

Figure 12 : Image grabbed with test vehicle

## 5. CONCLUSION

We have developed test vehicles in three different technologies - with same lithography (0.35µm) and same pixel pitch (15-13µm) - in order to compare performances of each of them. Use of improved and CIS processes have numerous advantages with regard to standard CMOS process. Quantum efficiency and dark current are better, and higher conversion gain can be reached. For standard technology, improvement can also be made by design optimization. Use of Nwell photodiode as photosensitive area in standard technologies permits to increase conversion gain and minimize dark current. For quantum efficiency, it appears that a technological optimization is the best way to improve it. Improvement

can be an optimization of superficial layers (passivation layer) or an addition of an anti-reflective film and adoption of dedicated doping profile for the photodiode.

Radiation tolerance results show that degradation can be dramatically reduced with radiation hard design techniques. Use of guard rings, ELT MOS or special buildings of photosensitive area allow to ensure good results with a minor of drawbacks.

In summary, the combination of process improvement that are already available - thanks to huge volume markets - and dedicated design techniques will allow for improved performances that can be used for the design of specific image sensor for space applications.

## ACKOWLEDGMENTS

The authors want to thank Celine Engel and Magali Estribeau (Supaero Integrated Image Sensors Laboratory) for numerous test vehicles characterizations and the ONERA Toulouse team for radiation facilities.

The authors are grateful to the CNES, especially to M.Laporte, and EADS-Astrium for financial and technical support.

## REFERENCES

1. M.Estribeau, P.Magnan, « Fast MTF measurement of CMOS imagers at the chip level using ISO 12233 slanted-edge methodology », SPIE Remote sensing 2004, Proceeding of SPIE, Vol.5570, September 2004.
2. Olivier Saint-Pé, Michel Tulet, Robert Davancens, Franck Larnaudie, Pierre Magnan, Philippe Martin-Gonthier, Franck Corbière, Pierre Belliot, Magali Estribeau, « Research-grade CMOS image sensors for remote sensing applications », SPIE Remote sensing 2004, Proceeding of SPIE, Vol.5570, September 2004.
3. M. Furumiya and al, « High sensitivity and No-Crosstalk pixel technology for embedded CMOS Image Sensor », IEEE TRANSACTIONS ON ELECTRON DEVICES, Vol. 48, NO. 10, October 2001.
4. H. Ihara and al, « A 3.7 x 3.7 $\mu m^2$ square pixel CMOS image sensor for digital still camera application », in ISSCC Tech. Dig., Feb. 1998, pp. 182-183.
5. O.-B. Kwon and al, « An improved digital CMOS imager », in Proc. IEEE Workshop Charge-Coupled Devices and Advanced Image Sensors, June 1999, pp. 144-147.
6. Bedabrata Pain, Thomas J. Cunningham, and Bruce Hancock, «Noise Sources and Noise Suppression in CMOS Imagers, Focal Plane Arrays for Space Telescopes » , Jet Propulsion Laboratory, California Institute of Technology, edited by Thomas J. Grycewicz, Craig R. McCreight, Proceedings of SPIE Vol. 5167 (SPIE, Bellingham, WA, 2004)
7. Hui Tian, Boyd Fowler, and Abbas El Gama*l,* «Analysis of Temporal Noise in CMOS Photodiode Active Pixel Sensor », IEEE JOURNAL OF SOLID-STATE CIRCUITS, VOL. 36, NO. 1, JANUARY 2001
8. P. Belliot, S. Basolo, F. Corbiere, P. Magnan, P. Martin-Gonthier, « Axe d'amélioration des performances de pixels de type APS réalisés en fonderie CMOS standard », CNES Workshop "APS & CCD", Novembre 2002
9. G. Anelli and al, « Radiation Tolerant VLSI Circuits in Standard Deep Submicron CMOS Technologies for the LHC Experiments :Practical Design Aspects », IEEE TRANSACTIONS ON NUCLEAR SCIENCE, Vol46, N°6, December 1999
10. B.R. Hancock, T.J.Cunningham, K. McCarty, G. Yang, C. Wrigley, P.G. Ringold, R.C. Stirbl, and B. Pain, « Multi-megarad (Si) radiation tolerant integrated CMOS imager », Jet Propulsion Laboratory, Proceeding of SPIE Vol. 4306, 2001
11. Gordon R. Hopkinson, « Radiation Effects in a CMOS Active Pixel Sensor », IEEE TRANSACTIONS ON NUCLEAR SCIENCE, VOL. 47, NO. 6, DECEMBER 2000